Molecular Medicine

Investigation on the Origin of Sperm DNA Fragmentation: Role of Apoptosis, Immaturity and Oxidative Stress

Monica Muratori,[1] Lara Tamburrino,[1] Sara Marchiani,[1] Marta Cambi,[1] Biagio Olivito,[2] Chiara Azzari,[2] Gianni Forti,[1] and Elisabetta Baldi[1]

[1]Sexual Medicine and Andrology Unit, Department of Experimental and Biomedical Sciences, Center of Excellence DeNothe, University of Florence, Italy; [2]Pediatric Section, Department of Health Sciences, University of Florence and Anna Meyer Children's University Hospital, Florence, Italy

Sperm DNA fragmentation (sDF) represents a threat to male fertility, human reproduction and the health of the offspring. The causes of sDF are still unclear, even if apoptosis, oxidative assault and defects in chromatin maturation are hypothesized. Using multicolor flow cytometry and sperm sorting, we challenged the three hypothesized mechanisms by simultaneously evaluating sDF and signs of oxidative damage (8-hydroxy, 2'-deoxyguanosine (8-OHdG) and malondialdehyde (MDA)), apoptosis (caspase activity and cleaved poly(ADP-ribose) polymerase (cPARP)) and sperm immaturity (creatine phosphokinase (CK) and excess of residual histones). Active caspases and c-PARP were concomitant with sDF in a high percentage of spermatozoa (82.6% ± 9.1% and 53.5% ± 16.4%, respectively). Excess of residual histones was significantly higher in DNA-fragmented sperm versus sperm without DNA fragmentation (74.8% ± 17.5% and 37.3% ± 16.6%, respectively, $p < 0.005$), and largely concomitant with active caspases. Conversely, oxidative damage was scarcely concomitant with sDF in the total sperm population, at variance with live sperm, where 8-OHdG and MDA were clearly associated to sDF. In addition, most live cells with active caspase also showed 8-OHdG, suggesting activation of apoptotic pathways in oxidative-injured live cells. This is the first investigation on the origin of sDF directly evaluating the simultaneous presence of the signs of the hypothesized mechanisms with DNA breaks at the single cell level. The results indicate that the main pathway leading to sperm DNA breaks is a process of apoptosis, likely triggered by an impairment of chromatin maturation in the testis and by oxidative stress during the transit in the male genital tract. These findings are highly relevant for clinical studies on the effects of drugs on sDF and oxidative stress in infertile men and for the development of new therapeutic strategies.

Online address: http://www.molmed.org
doi: 10.2119/molmed.2014.00158

INTRODUCTION

In the last two decades we have been aware that in human ejaculates there can be high percentages of sperm with DNA fragmentation, representing a threat for male fertility, human reproduction and the health of the offspring. In addition, in the era of assisted reproduction techniques (ARTs) which bypass many, if not all, natural barriers to fecundation, the risk that sperm with unresolved DNA damage can fertilize an oocyte (1) appears increased, thus raising further concerns on the presence of DNA breaks in the sperm genome. The first reports on sperm DNA fragmentation (sDF) date back to the late 1980s (2) and early 1990s (3) and, since then, the biological and clinical meanings of this type of sperm damage have been investigated extensively and several techniques to reveal it have been developed (4). However, the causes and the sites of origin of sDF have not been completely clarified and, still, we are dealing with hypotheses and theories. Clearly, the knowledge of the mechanisms responsible for this type of sperm damage is pivotal for the development of effective treatments to prevent the onset of sDF in infertile men.

Besides well-known external inducers of sDF, including chemotherapy (5), environmental toxicants (6) and the presence of leukocytes in semen (7), three main mechanisms have been proposed to explain the genesis of sDF. According to one of these proposed mechanisms, the DNA nicks occurring to promote the remodeling of sperm chromatin are not completely repaired due to an impairment of the sperm maturation process (8,9). sDF also could reflect a DNA cleav-

Address correspondence to *Monica Muratori and Elisabetta Baldi, Sexual Medicine and Andrology Unit, Department of Experimental, Clinical and Biomedical Sciences, University of Florence, Florence Viale Pieraccini, 6 I-50139 Firenze Italy. Phone: +39-055-2758235; E-mail: monica.muratori@unifi.it or elisabetta.baldi@unifi.it.*
Submitted August 7, 2014; Accepted for publication January 30, 2015; Published Online (www.molmed.org) January 30, 2015.

age produced by a process of apoptosis first triggered and later interrupted in the testis (that is, abortive apoptosis) (10) or occurring after spermiation (11,12). Finally, sperm DNA breaks could be provoked by attacks of free radicals, including reactive oxygen species (ROS) (13), acting both in testis and in posttesticular sites (14,15). It is anticipated that these proposed mechanisms are not alternative, but can concur in generating the sperm DNA damage. Indeed, besides the occurrence of persistent DNA nicks, an impairment in chromatin maturation could produce poorly compacted nuclei, which are more vulnerable to oxidative assault (13). Similarly, ROS could break the DNA backbone directly, but also act as triggers of apoptotic pathways ending in caspases and apoptotic nucleases activation, as happens in somatic cells (16). The above hypotheses are supported by indirect studies showing that infertile/subfertile subjects who are known to have increased levels of sDF show higher degrees of cell immaturity (17) or of apoptotic features (18–20) or of oxidative stress (21,22) in their ejaculates and by correlative studies reporting associations between the levels of sDF and signs of impaired chromatin maturation, (23,24) or apoptotic traits (25,26) or evidence of oxidative stress (27,28). However, these approaches detect the markers of the hypothesized mechanisms in different semen aliquots from those used to reveal sDF and the occurrence of statistical correlations does not necessarily imply a cause–effect relationship. Only in a few studies (24,28) has a direct approach been used to study the mechanisms responsible for sDF by double-staining sperm for sDF and chromatin immaturity markers. In such studies (24,28), the latter are strictly linked to sperm DNA breaks as observed in a small number of cells by microscopy. Sakkas *et al*. (29) employed flow cytometry to address the relation between sDF and apoptotic proteins, failing, however, in revealing a link between sperm DNA breaks and apoptosis, possibly because of the inclusion in the fluorescence analyses of semen apoptotic bodies, scarcely TUNEL-labeled (30) but highly expressing apoptotic features (31).

In the present study, we challenged the hypothesized mechanisms and their relative contribution to the genesis of sDF by directly investigating the presence of signs of apoptosis, chromatin immaturity and oxidative stress in a large number of sperm with and without DNA fragmentation. To this aim, we used multicolor flow cytometry to simultaneously detect sDF and signs of oxidative damage (8-hydroxy, 2′-deoxyguanosine [8-OHdG] and malondialdehyde [MDA]), of apoptosis (active caspases and cleaved poly[ADP-ribose] polymerase [cPARP]) and of sperm immaturity (creatine phosphokinase [CK]) (32,33). The association between sDF and chromatin immaturity also was investigated by aniline blue (AB) staining in fractions of sperm with and without sDF, separated by fluorescence-activated cell sorting. To our knowledge, this is the first study on the origin of sDF where the concomitance of this sperm damage with the possible causes responsible for it was investigated by a high throughput strategy.

MATERIALS AND METHODS

Chemicals

Human tubal fluid (HTF) medium was purchased from Celbio (Milan, Italy). Bovine serum albumin (BSA) was purchased from ICN Biomedicals (Irvine, California, USA). The primary antibodies used in the study were: monoclonal mouse antibodies anti 8-OHdG, 15A3 (Santa Cruz Biotechnology, Santa Cruz, CA, USA) and anti MDA, clone 1F83 (JaICA, Haruoka, Japan); CKB antibody (N-term), purified rabbit polyclonal antibody (Abgent, San Diego CA, USA). Antibodies for secondary detection were: the goat anti-rabbit IgG (H + L chain specific), fluorescein (FITC) conjugate (Southern Biotech, Birmingham, AL, USA); the goat anti-mouse IgG-FITC and the sheep anti-mouse IgG (whole molecule) F(ab′)2 fragment–R-phycoerythrin (R-PE) (Sigma-Aldrich, St. Louis, Missouri, USA). Mouse IgG2a isotype control antibody was purchased from Exbio (Praha, Czech Republic). Anti-PARP CSSA FITC, apoptosis detection kit and Vybrant FAM Caspase-3 and -7 Assay Kit were purchased from Life Technologies (Paisley, UK [Thermo Fisher Scientific Inc., Waltham, MA, USA]).

Ethics Statement

The study has been approved by the Local Ethical Committee of the Azienda Ospedaliera e Universitaria (AOUC) Careggi, and informed written consensus has been obtained from the recruited patients.

Semen Sample Collection

Semen samples were consecutively collected according to WHO criteria (34) from men undergoing routine semen analysis as part of testing of couples with fertility problems in the Andrology Laboratory of the University of Florence. Subjects undergoing drug therapies were excluded from the study as well as semen samples where leukocytes exceeded 1 million/mL. Occurrence of leukocytes was assessed by counting all round cells in the Neubauer chamber and then distinguishing leukocytes from germ cells after differential quick staining of the sample. For the experiments of the study, semen samples were processed individually and different semen samples were used for each marker. Overall, we recruited 92 subjects (average age: 34.8 ± 7.8 years) showing the following average semen parameters values: normal morphology, 6.2 ± 4.8%; total motility, 60.5 ± 20.9%; progressive motility, 56.7 ± 14.5%; concentration, 70.6 ± 41.8 millions/mL; total number/ejaculate, 288.1 ± 137.5 millions. After liquefaction (30 min following collection according to [34]), semen samples were washed twice with HTF medium and, treated by dithiothreitol (DTT, 2 mmol/L, 45 min at room temperature) (35), washed again twice with the same medium and, unless otherwise indicated, fixed by 500 μL of 4% paraformaldehyde in phosphate buffered saline (PBS), pH 7.4, for 30 min at room temperature.

For experiments of treatment of sperm with H_2O_2, semen samples were washed twice and split into two aliquots that were incubated in the medium containing or not 5 mmol/L H_2O_2 for 2 h at 37°C (36). After washing, samples were then treated by DTT and fixed as described above.

For experiments in live sperm, after washing with HTF medium, fresh semen samples were incubated for 1 h at room temperature, in the dark, in 500 μL of PBS with LIVE/DEAD Fixable Far Red Dead Cell Stain Kit (L10120, diluted 1:10 000; Life Technologies [Thermo Fisher Scientific]), and treated with DTT and fixed as described above. L10120 is able to bind dead cells and the labeling is stably kept in the cells after sample fixation and permeabilization (35,37,38).

TUNEL Assay

For labeling sDF, samples were processed by terminal deoxynucleotidyl transferase (TdT)-mediated fluorescein-dUTP nick end labeling (TUNEL) as described elsewhere (39). Briefly, fixed sperm were washed by PBS/BSA 1% twice and permeabilized with 0.1% Triton X-100 in 100 μL of 0.1% sodium citrate for 4 min in ice. After washing two times, the labeling reaction was performed by incubating sperm in 50 μL of labeling solution (supplied with the In Situ Cell Death Detection Kit, fluorescein, Roche Molecular Biochemicals, Milan, Italy) containing the TdT enzyme, for 1 h at 37°C in the dark. Finally, samples were washed twice, resuspended in PBS, stained with PI (propidium iodide, 0.75 μg/mL) and incubated in the dark for 15 min at room temperature. For each test sample, a negative control was also prepared by omitting TdT.

Positive controls for TUNEL were prepared: (i) by incubating sperm with 2 mmol/L H_2O_2 in HTF medium (3 h, 37°C) before processing samples for TUNEL; (ii) by treating sperm with DNAse I (Pharmacia Biotech Italia, Milan, Italy), 2 IU for 20 min at 37°C, before the labeling reaction.

In preliminary experiments, we assessed whether the pretreatment of samples with DTT increased the sensitivity of TUNEL. In agreement with a previous study (35), we found that DTT treatment increased the percentage of sDF from 31.8 ± 15.8% to 37.9 ± 19.0% ($p < 0.01$, n = 10).

Simultaneous Detection of Oxidative Signs (8-OHdG and MDA) and sDF

Fixed sperm (20×10^6) were washed (twice with 1% normal goat serum [NGS]-PBS) and split into two aliquots. For 8-OHdG detection, the two aliquots were incubated in 100 μL of 0.1% sodium citrate/0.1% Triton X-100 containing 2 μg/mL anti-8-OHdG antibody 15A3 (test sample) or 2 μg/mL mouse IgG2a (isotype control) for 1 h at 37°C (40). For MDA detection, the aliquots were first permeabilized in 100 μL of 0.1% sodium citrate/0.2% Triton X-100 (30 min at room temperature) and then incubated in 100 μL of 1% NGS-PBS containing 2 μg/mL of the antibody against MDA (test sample) or 2 μg/mL mouse IgG2a (isotype control) for 1 h at 37°C (41). After incubating with the antibodies and washing twice with 1% NGS-PBS, sperm were incubated in the dark (1 h at room temperature) with FITC-conjugated goat anti-mouse IgG (dilution 1:100 in 100 μL 1% NGS-PBS). Then, both the test sample and the isotype control were split again into two aliquots and each aliquot was processed for TUNEL assay as described above. However, to avoid the overlapping between fluorescence signals emission, we used TMR (tetramethylrhodamine)-conjugated dUTPs (39) supplied with the In Situ Cell Death Detection Kit, TMR (Roche Molecular Biochemicals). For similar reasons, nuclear staining was performed by DAPI (1 μg/mL for 15 min in the dark at room temperature) instead of PI. DAPI staining is able to discriminate between M540 bodies and sperm and, within the latter, between brighter and dimmer populations (see Results section) similarly to PI staining. Indeed, in preliminary experiments (n = 5 semen samples) we found that the percentages of sperm within the flame-shaped region in forward scatter/side scatter (FSC/SSC) dot plots (see below) and of the two populations versus total sperm do not change by staining with DAPI and PI (data not shown).

In some experiments (n = 3), we assessed the reproducibility of the above procedures by processing semen samples in duplicate and comparing the two measures. In the case of 8-OHdG/TUNEL, we found an average coefficient of variation (CV) of 4.9% ± 5.0% for TUNEL and of 2.1% ± 1.0% for 8-OHdG. In the case of MDA/TUNEL, the average CV of the measures was 7.9% ± 3.9% for TUNEL and 19.2% ± 15.1% for MDA.

We also verified whether the double-labeling procedure affected the measures of each parameter as if separately determined. Regarding TUNEL/MDA detection, the average CVs of the measures obtained by double and single labeling were 12.1% ± 1.0 %, (n = 3) for TUNEL and 20.0% ± 5.5%, (n = 3) for MDA. Similarly, the measures of sDF as assessed by double (TUNEL/8-OHdG) and single labeling were fairly consistent (average CVs = 7.9% ± 1.5% and 4.9% ± 5.4%, respectively, for TUNEL and 8-OHdG, n = 3).

Simultaneous Detection of CK and sDF

For CK detection (33), fixed sperm (20×10^6) were washed (twice with 1% NGS-PBS) and permeabilized in 100 μL of 0.1% sodium citrate/0.1% Triton X-100 for 4 min in ice. After washing with 1% NGS/PBS, sperm were blocked for 20 min in 5% NGS in PBS and washed again. Then the samples were split into two aliquots and incubated in 100 μL of 1% NGS–PBS containing 5 μg/mL of the antibody against CK (test sample) or 5 μg/mL of anti-rabbit serum (negative control) for 1 h at room temperature. After washing twice with 1% NGS-PBS, sperm were incubated in the dark (1 h at room temperature) with the FITC-conjugated goat anti-rabbit IgG (1:100 in 100 μL of 1% NGS/PBS). Finally, samples were washed twice and both the sample test and the negative control were further split into two aliquots and each aliquot was processed for TUNEL assay as described above, using TMR-dUTPs for the labeling of DNA breaks and DAPI for nuclear staining.

In some experiments (n = 3), we assessed the reproducibility of the above procedure by processing semen samples in duplicate and comparing the two measures. We found an average CV of 12.4% ± 5.1% for TUNEL and of 14.9% ± 19.7% for CK expression.

We also verified whether the double-labeling procedure affected the measures of each parameter as if separately determined. The average CVs of the measures obtained by double TUNEL/CK labeling and single labeling were 14.9% ± 6.8% (n = 3) for TUNEL and 7.1% ± 1.6% (n = 3) for CK.

Simultaneous Detection of cPARP and sDF

For detection of cPARP (12), we used the FITC-conjugated anti-PARP cleavage site-specific antibody (CSSA) kit, following the instructions of the manufacturer, with slight modifications. Briefly, washed sperm samples (15×10^6) were fixed in 1 mL IC Fix buffer for 20 min at 4°C and, after washing twice and resuspension in PBS/BSA1%, split into two aliquots for negative control and test sample. In the latter, 10 μL of the antibody anti-cPARP were added and then the aliquots were incubated for 30 min at room temperature. After washing, the sample test and the negative control were split into two aliquots and each aliquot was processed for TUNEL assay as described above using TMR-dUTPs for the labeling of DNA breaks and DAPI for nuclear staining.

In some experiments (n = 3), we assessed the reproducibility of the above procedure by processing semen samples in duplicate and comparing the two measures. We found that the average CV of the measures was 12.1% ± 3.9% for TUNEL and 15.5% ± 10.2% for cPARP.

We also verified whether the double labeling procedure affected the measures of each parameter as if separately determined. The average CVs of the measures obtained by double TUNEL/PARP labeling and single labeling were 3.5% ± 2.9% (n = 3) for TUNEL and 6.3% ± 3.3% (n = 3) for PARP.

Simultaneous Detection of Active Caspases and sDF

Caspases were evaluated by Vybrant FAM Caspase-3 and -7 Assay Kit which detects active caspases 3 and 7 by using the FAM-DEVD-FMK reagent (FLICA), a fluorescent-labeled inhibitor of such enzymes that covalently binds the enzymatic reactive center of the activated caspases (31). Briefly, sperm samples (15×10^6) were resuspended in HTF medium and split into two aliquots for the negative control and the test sample. In the latter, 10 μL of 30× FLICA working solution was added, then aliquots were incubated for 1 h at 37°C in the dark. After two washes with wash buffer 1× (included in the kit mentioned above), samples were fixed by adding 40 μL of 10% formaldehyde solution (included in the kit mentioned above) for 10 min at room temperature. Then, sperm samples were washed again twice and both negative control and test sample were split again into two aliquots that were processed for TUNEL assay as described above, using TMR-dUTPs for the labeling reaction and DAPI for nuclear staining.

In selected experiments we investigated the concomitance of 8-OHdG and active caspases in live sperm. To this end, after labeling with L10120, sperm samples were processed for detection of caspase activity by the above procedure. Then, both the negative control and test sample were split into two aliquots that, in turn, were labeled for 8-OHdG detection as described above, but using an antibody conjugated with R-PE for secondary detection to avoid fluorescence of 8-OHdG that overlapped that of FLICA.

In some experiments (n = 3), we assessed the reproducibility of the above procedure by processing semen samples in duplicate and comparing the two measures. We found that the average CVs of the measures were 4.5% ± 5.5% for TUNEL and 4.7% ± 3.8% for activated caspases.

We also verified whether the double-labeling procedure affected the measures of each parameter as though separately determined. The average CVs of the measures obtained by double TUNEL/FLICA labeling and single labeling were 20.2% ± 2.8 % (n = 3) for TUNEL and 26.3% ± 1.7%, (n = 3) for FLICA.

Flow Cytometry

All flow cytometric analyses were conducted by a FACSAria II flow cytometer (BD Biosciences, San Jose, CA, USA) equipped with a violet laser, a blue laser and a red laser for excitation at 405 nm, 488 nm and 633nm, respectively. Before acquiring, sperm were filtered by 50 μm Syringe Filcons (BD Biosciences). For each sample, 8,000 events were recorded within the gate including DAPI- (or PI) stained cells of the characteristic flame-shaped region (FR in Figure 1) in the FSC/SSC cytograms (39). In samples previously stained with L10120, 8,000 live sperm were recorded. Blu (DAPI), green (FITC), red (TMR, PI and R-PE) and far red (L10120) fluorescence was revealed by PTMs equipped with 450/40, 530/30, 585/42 and 660/20 BP filters, respectively. In multicolor flow cytometric analyses, fluorescence compensation was set by single-stained cellular controls that were prepared for each color and each semen sample (see also the above procedures of simultaneous detection of sDF and apoptosis/oxidative stress/immaturity in DAPI-stained sperm). BD FACSDiva Software (BD Biosciences) was used for acquisition and data analysis. Sperm were gated by the characteristic flame-shaped region in FSC/SSC dot plots and, within it, by the region containing nuclear-labeled events (39). For experiments conducted in live sperm, we further gated L10120 unstained sperm and within such population we (i) calculated the percentage of TUNEL positivity and (ii) studied the concomitant presence of sDF and 8-OHdG or MDA or active caspases and of 8-OHdG and active caspases.

Fluorescence-Activated Cell Sorting

Fluorescence-activated cell sorting was used to separate TUNEL-positive

from TUNEL-negative sperm. Samples containing double-labeled PI/TUNEL sperm were adjusted at concentration of 10^7cells/mL, filtered by 50-μm Syringe Filcons and immediately sorted by the BD FACSAria II cell-sorting system equipped with a FACSSort fluid sorting module. For sperm sorting, we used the followings settings: laser power, 13 mW; nozzle, 70 μm; sort setup, low; sheath pressure, 34.50 psi; frequency, 60.0 kHz; flow rate, 1–3 μL/min (maximum of 7,000 events/second); and precision, 0160. After gating to exclude large cells, debris and other semen interference (39), as described above, we used the negative control (omitted TdT) as reference for drawing two regions around the TUNEL negative and positive sperm. After sorting, we acquired the sorted fractions again by flow cytometry to check the purity of sperm with and without DNA fragmentation.

Staining with Aniline Blue (AB)

To evaluate sperm chromatin immaturity, we performed AB labeling (24,42). Briefly, after sperm sorting as described above, 100,000 sperm were smeared on slide, air dried and then stained with 5% aqueous AB (Sigma-Aldrich) mixed with 4% acetic acid (pH 3.5) for 5 min (42) at room temperature. Two hundred sperm were analyzed on each slide under a light microscope (Leica DM LS, Leica, Wetzlar, Germany). Sperm showing dark-blue staining were considered as AB positive, whereas those stained only weakly or not at all were considered as AB negative (43). After determining the percentage of fragmented sperm in presorted samples, the overall percentage of AB staining in such samples was calculated by (% AB staining in fragmented sperm × % fragmented sperm)/100 + (% AB staining in nonfragmented sperm × % nonfragmented sperm)/100.

Fluorescence Microscopy

Sperm labeled for sDF and for 8-OHdG, MDA, CK, active caspases or cPARP as described above, were spread onto slides and mounted with fluoromount aqueous mounting medium (Sigma Aldrich). Green and red fluorescence was examined using a fluorescence microscope (Axiolab A1 FL, Carl Zeiss, Milan, Italy), equipped with Filter set 15 and 44 by an oil immersion 100× magnification objective.

Statistical Analyses

All variables were checked for normal distribution by the Kolgomov-Smirnov one-sample test. Since all variables resulted as normally distributed, results are expressed as mean ± SD and analysis of variance and the Student *t* test (paired and unpaired data) were used to assess statistically significant differences between the compared groups. A *p* value of 0.05 was considered as statistically significant. Coefficients of variation were calculated by (SD/mean) × 100. All statistical analyses were carried out using MicroCal Origin software, 6.1 version (MicroCal Software Inc., Northampton, MA, USA) except for evaluation of normal distribution, which was obtained by using SPSS software, 20 version, for Windows (SPSS [IBM, Armonk, NY, USA]).

All supplementary materials are available online at www.molmed.org.

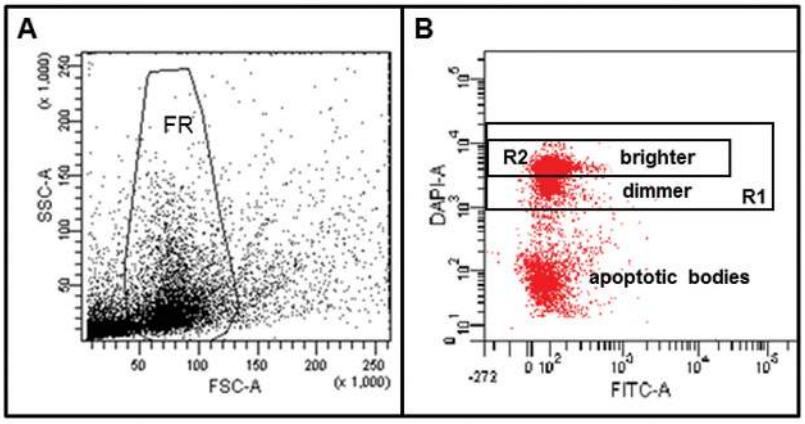

Figure 1. (A) Typical FSC/SSC dot plot of a semen sample showing the flame-shaped region (FR) containing semen apoptotic bodies and sperm. The latter are defined by nuclear staining with DAPI (B), that also distinguishes two sperm populations named brighter and dimmer because of the different intensity of nuclear staining. Total sperm population is included in R1 region, whereas brighter sperm are in R2 region.

RESULTS

Multicolor Flow Cytometry

To study the simultaneous occurrence of apoptosis, immaturity and oxidative damage in sperm with sDF, we used flow cytometry to evaluate specific markers of each of the three processes in sperm samples stained by TUNEL and DAPI. Supplementary Figure 1 reports a flow chart depicting the experimental sets of the study. The staining with DAPI (Figure 1B) is necessary to define the sperm population (44) within the FSC/SSC region (Figure 1A), containing both sperm and semen apoptotic bodies lacking chromatin (31). Nuclear staining also unveils the occurrence of two sperm populations, named brighter and dimmer populations, based on a different intensity of such staining (44) (see Figure 1B). Brighter population represents the majority of semen sperm showing a normal DNA content (42), albeit fragmented in a variable percentage (44), whereas dimmer population represents roughly 15% of sperm and is totally composed by DNA-fragmented (44) and dead (45) cells, including those with large loss of chromatin material (41). Hence, data presented here, albeit referred to the total sperm population (region R1 in Figure 1B) unless other-

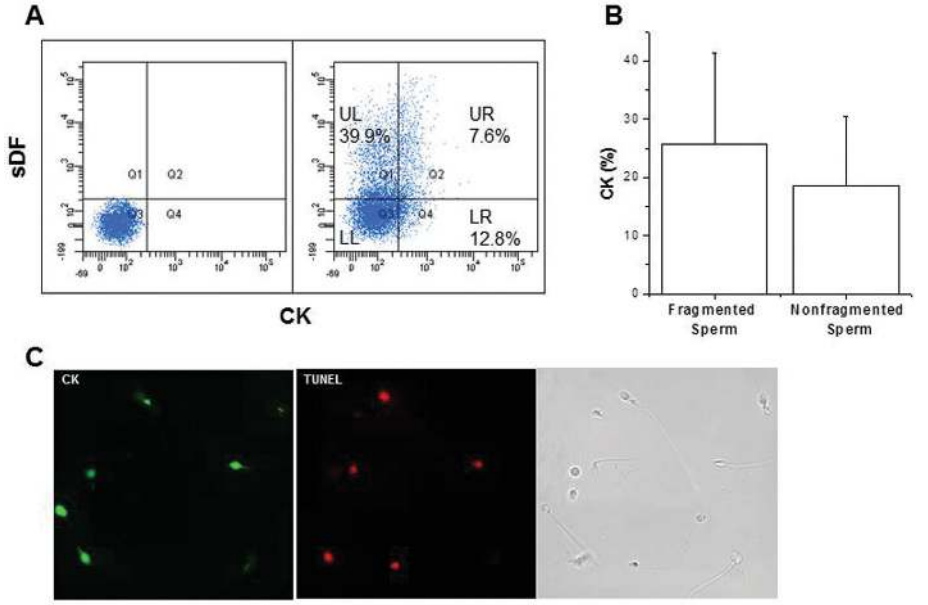

Figure 2. Concomitance of sDF and CK in human spermatozoa. (A) Dot plots of the negative control (left panel) and the corresponding test sample (right panel) showing the percentages of sperm without sDF and CK (LL quadrant), sperm with sDF and without CK (UL quadrant), sperm with sDF and CK (UR quadrant) and sperm without sDF and with CK (LR quadrant). Representative of nine experiments. Percentages in the quadrants refer to the shown sample. (B) Percentage of CK in fragmented (UR/(UR + UL)) and nonfragmented (LR/(LL + LR)) sperm. (C) Images from fluorescence microscopy showing the localization of CK (left panel) in sperm with and without TUNEL labeling (middle panel). Right panel: bright field. Original magnification 1,000×. LL, lower left; UL, upper left; LR, lower right; UR, upper right.

wise indicated, also were determined by excluding dimmer sperm (that is, in the only brighter population, region R2 in Figure 1B).

Association of sDF with Sperm Immaturity

Expression of CK. To study the role of immaturity in the origin of sDF, we investigated the expression of the marker of cytoplasmic retention, CK (32,33), by detecting the enzyme with an immunofluorescent technique (Figure 2A). In semen samples stained for sDF and CK, we found that, on average, 19.0% ± 11.8% of sperm shows this trait of immaturity and that this cytoplasmic enzyme is present in cells with and without DNA fragmentation in similar amounts (see Figure 2A). In Supplementary Table 1, the average percentages of sperm in the four quadrants of Figure 2A (right panel, presence and absence of CK in sperm with and without sDF), as observed in nine different samples, are shown. To understand whether CK is preferentially expressed in sperm with sDF, we calculated the percentage of sperm expressing CK within the DNA-fragmented and the nonfragmented sperm. We found no difference in the presence of CK in the two groups of sperm (Figure 2B). Similar results were obtained when only brighter sperm were considered (brighter sperm expressing CK: 26.8% ± 15.7 % in DNA-fragmented fraction versus 18.4% ± 11.9% in nonfragmented, $p > 0.05$). Images by fluorescence microscopy of double-stained sperm for sDF and CK are reported in Figure 2C. As can be observed, the enzyme was localized in the head, in the midpiece or both, as reported previously (33).

Sperm sorting and aniline blue staining (AB). The relationship between sDF and immaturity also was investigated by verifying whether sperm with DNA breaks show a larger persistence of histones as a result of an incomplete chromatin maturation. To this aim, we stained sperm with AB that selectively binds lysine-rich histones (24,43). In these experiments, we excluded dimmer sperm, as we suspected that AB underestimates chromatin immaturity in such populations due to their massive loss of chromatin material (42). After labeling with TUNEL, we sorted brighter sperm with and without sDF and, in samples where the separation was successful (Figure 3A), we stained the two fractions with AB. The score of AB staining in the sorted fractions indicated that the percentage of sperm with chromatin immaturity (dark blue, Figure 3B) is much greater in the fraction of cells with DNA breaks as compared to sperm with intact DNA (Figure 3C and Supplementary Figure 2, which shows raw data of single experiments). A rough calculation of AB staining in the entire brighter population yielded a result of about 50%, consistent with previous results (42).

Association of sDF with Apoptosis: Caspase Activation and cPARP

To investigate whether sDF associates with apoptosis, we simultaneously detected the fluorescence of TUNEL and that of FLICA revealing activated caspases 3 and 7 (effector caspases) (46). We found that nearly all sperm with sDF also expressed these apoptotic enzymes (Figure 4A). However, active caspases (overall occurring in 32.8% ± 14.0% of sperm, n = 13) also were present, albeit at a lesser extent, in sperm without DNA damage (Figure 4A and Supplementary Table 1). Consistently, in sperm with sDF, the percentage of apoptotic cells was significantly greater than in nonfragmented sperm (Figure 4B), suggesting a sharp association between the two phenomena. The same strict association also was observed when considering only brighter sperm (percentage of apoptosis in fragmented sperm: 83.3% ± 10.0% versus 15.3% ± 9.8% in nonfragmented, n = 13, $p < 0.0001$). Images collected by fluores-

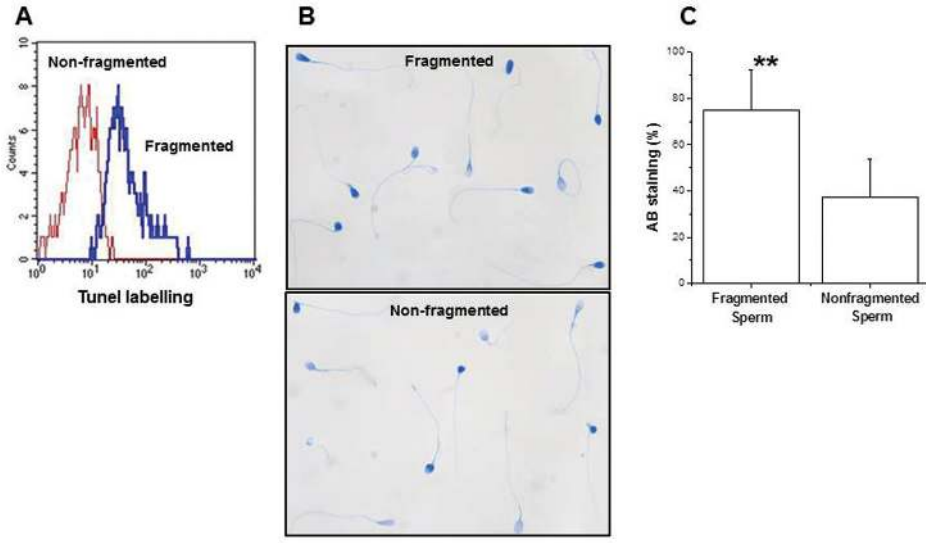

Figure 3. Sorting fragmented and nonfragmented sperm by FACSAria II and staining with AB (n = 5). (A) TUNEL fluorescence histograms of the sorted fragmented and nonfragmented sperm. (B) Staining with AB of the sorted fractions. Sperm nuclei with intense dark-blue staining were considered to be immature. Original magnification 1,000×. (C) Percentage of chromatin immaturity, as detected by AB staining, in fragmented and nonfragmented sperm. $^{**}p < 0.01$.

cence microscopy of sperm processed for both TUNEL and caspases show that the apoptotic enzymes (Figure 4C, left panel) localize in the post acrosomal region of the head and in the midpiece, consistent with previous results (25,46).

The association between sDF and apoptosis also was investigated by using another apoptotic marker, the cleaved form of PARP (cPARP), (12,47). Figure 5A reports a typical dot plot showing the immunofluorescent detection of cPARP in TUNEL-labeled sperm. Similarly to results with caspases, a great overlapping of the two parameters was observed. Again, a fraction of TUNEL-negative sperm exhibiting the apoptotic protein was present (Figure 5 and Supplementary Table 1). Overall, cPARP was detected in 28.4% ± 13.0 % of sperm (n = 10), and was clearly associated to sDF with a significant higher proportion in TUNEL-positive sperm ($p < 0.001$, Figure 5B). The same result was obtained in brighter sperm, (52.8% ± 14.3% in DNA-fragmented versus 20.7% ± 12.7% in nonfragmented, $p < 0.0001$). By fluorescence microscopy, we found that cPARP was localized in the head and midpiece (Figure 5C, left panel) of sperm, as reported previously (48).

Association of sDF with Oxidative Damage: 8-OHdG and MDA

The association between sDF and oxidative damage was studied by evaluating 8-OHdG, the hallmark of oxidative DNA damage, with an immunofluorescence technique that we previously demonstrated to reveal specifically the oxidized base in sperm nuclei (40). In 21 semen samples labeled for 8-OHdG and TUNEL (Figure 6A), 11.7% ± 5.6% of sperm, on average, showed the oxidized guanosine, consistent with our previous study (40). The oxidative DNA damage was concomitantly present with sDF only in small percentages of sperm, as most oxidized sperm did not show DNA breaks (Figure 6A and Supplementary Table 1). Further, the incidence of sperm with 8-OHdG in DNA-fragmented cells was not statistically different from that of cells without sDF (Figure 6B, left panel). However, when we considered only brighter sperm, a link between sDF and oxidative damage was unveiled, as the occurrence of guanosine oxidation was significantly greater in the fragmented cells (Figure 6B, right panel). Although several reports demonstrate that induction of DNA damage in sperm by oxidative insult is detected by TUNEL assay (35,49–51), a recent study questions this possibility (36). Thus, the absence of a clear association between direct oxidative damage and DNA fragmentation (Figure 6) may be ascribed to lack of ability of TUNEL assay to detect oxidative DNA fragmentation. To exclude this possibility, we treated semen samples with H_2O_2 for 2 h and evaluated sDF by TUNEL. We found an increase (51.4% ± 9.1% in treated samples versus 22.2% ± 1.7% in untreated, $p < 0.05$, n = 3) of sDF, demonstrating that, in our hands, TUNEL assay is able to reveal DNA fragmentation induced by oxidative stress *in vitro*.

The association between DNA breakage and oxidative insult was studied further by detecting another marker, the product of lipid peroxidation MDA, by using an immunofluorescent technique. The simultaneous staining for TUNEL and MDA showed, on average, a percentage of 17.7 ± 7.9 sperm (n = 11) with MDA and depicted a pattern of association of the two parameters similar to that with 8OHdG (compare Figure 6A and 6C). Indeed, the concomitance between expression of MDA and sDF was found in a small percentage of sperm, with most damaged sperm exhibiting sDF and MDA alternatively (Figure 6C and Supplementary Table 1). The incidence of sperm with MDA among those fragmented and nonfragmented was not statistically different (Figure 6D, left panel). However, as for 8OHdG (Figure 6B, right panel) the link between the membrane oxidative damage and DNA breaks became evident when we considered only the brighter sperm (Figure 6D, right panel). MDA was mostly localized in the midpiece of sperm (Figure 6E, left panel) (52).

Association of sDF with 8-OHdG, MDA and Active Caspases in Live Sperm

From the above data, it appears that the association between oxidative damage

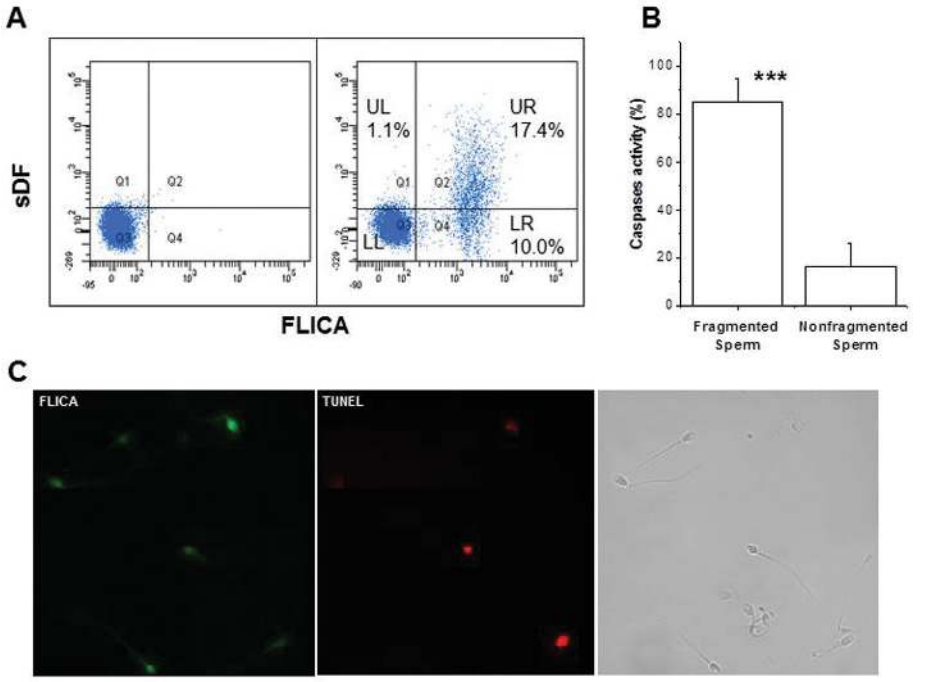

Figure 4. Concomitance of sDF and active caspases in human spermatozoa. (A) Dot plots of the negative control (left panel) and the corresponding test sample (right panel) showing the percentages of sperm without sDF and active caspases (LL quadrant), sperm with sDF and without active caspases (UL quadrant), sperm with sDF and caspase activity (UR quadrant) and sperm without sDF and with active caspases (LR quadrant). Representative of 13 experiments. Percentages in the quadrants refer to the shown sample. (B) Percentage of sperm with active caspases in fragmented (UR/(UR + UL)) and nonfragmented (LR/(LL + LR)) sperm. (C) Images from fluorescence microscopy showing the localization of active caspases (left panel) in sperm with and without TUNEL labeling (middle panel). Right panel: bright field. Original magnification 1,000×. ***$p < 0.001$. LL, lower left; UL, upper left; LR, lower right; UR, upper right.

and sDF occurs when considering only brighter sperm, that is, excluding the fragmented and dead dimmer ones (38,44). This finding suggests that the role of oxidative species in generating sDF might be more evident in live sperm and prompted us to investigate the association between oxidative damage and sDF in only live sperm, where the damage is still ongoing. To this aim, we processed samples after labeling with L10120 to mark dead cells and exclude them from the flow cytometric analyses (35,37,38). In the 19 studied patients, the amount of DNA fragmentation was 14.6% ± 10.5% in live and 59.9% ± 16.7% in dead sperm. Simultaneous detection of sDF with 8-OHdG and MDA (Figures 7A, B), showed that the mean percentages of live sperm with the oxidative damage were 18.4 ± 9.2 (n = 6) for 8-OHdG and 46.7 ± 14.4 for MDA (n = 6), indicating that signs of oxidative stress are more pronounced in live sperm with respect to the total population (Supplementary Table 1). Concomitance of sDF with 8-OHdG and MDA was present, respectively, in 4.0% ± 2.4% and 10.8% ± 7.0% sperm. In addition, the incidence of both oxidative markers was statistically higher in fragmented sperm than in nonfragmented ones (Figures 7A, B, lower panels). We also investigated the concomitance of sDF and caspase activation in live sperm. We found that the apoptotic marker is concomitant with sDF in 5.2% ± 2.7% of live sperm (n = 7), whereas 4.5% ± 2.5% of them showed only the apoptotic trait. The percentage of active caspases in live fragmented sperm was significantly greater than in nonfragmented (Figure 7C, lower panel) and was not different ($p > 0.05$) from that calculated for either 8-OHdG (see Figure 7A, lower panel) or MDA (see Figure 7B, lower panel).

The above results suggest that oxidative and apoptotic signs can be concomitant in live sperm. To investigate this possibility, we simultaneously evaluated 8-OHdG and caspase activity in live sperm in three semen samples. As shown in Figure 7D, whereas most oxidized sperm did not show the apoptotic enzymes, most caspase-positive sperm also exhibited the 8-OHdG.

DISCUSSION

Understanding the causes of sDF is a goal sought over the last two decades, given the crucial importance of DNA integrity of spermatozoa for human reproduction and the health of the offspring. Using mostly multicolor flow cytometry analyses, we obtained postejaculation snapshots of how apoptosis–oxidation–immaturity (the three hypothesized mechanisms generating sDF) are distributed in total and live sperm with or without sDF, from which we can infer the pathways leading to such damage. Based on our results, the following conclusions can be drawn: (i) apoptosis is the main pathway leading to DNA breakage in sperm; (ii) chromatin immaturity induces sDF through activation of an apoptotic pathway; and (iii) oxidative attack appears to act after spermiation, occurring mostly in live sperm.

The finding that nearly all sperm with sDF also show the activity of the effector caspases 3 and 7 strongly indicates a key role of apoptosis in generating the bulk of sperm DNA breaks, consistent with the reported correlations between the levels of DNA breakage and of apoptotic traits in sperm (25,26). In addition, the causative relation between caspase activation and sDF also is suggested by the presence of a certain percentage of cells with the apoptotic enzymes but without DNA breaks, consistent with the idea

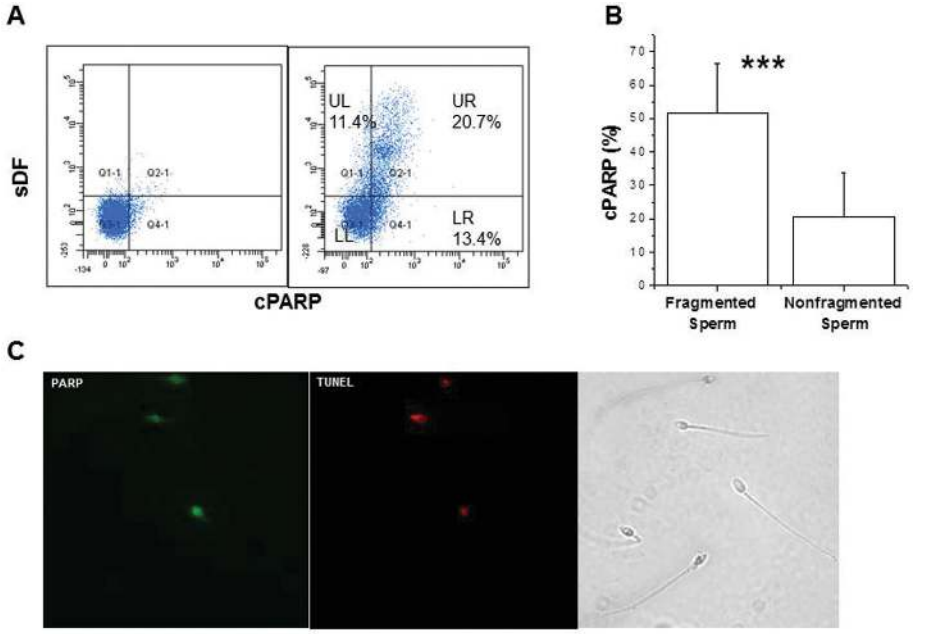

Figure 5. Concomitance of sDF and cPARP in human spermatozoa. (A) Dot plots of the negative control (left panel) and the corresponding test sample (right panel) showing the percentages of sperm without sDF and cPARP (LL quadrant), sperm with sDF and without cPARP (UL quadrant), sperm with sDF and cPARP (UR quadrant), sperm without sDF and with cPARP (LR quadrant). Representative of 10 experiments. Percentages in the quadrants refer to the shown sample. (B) Percentage of sperm with cPARP in fragmented (UR/(UR + UL)) and nonfragmented (LR/(LL + LR)) sperm. (C) Images from fluorescence microscopy showing the localization of cPARP (left panel) in sperm with and without TUNEL labeling (middle panel). Right panel: bright field. Original magnification 1,000×. ***$p <$ 0.001. LL, lower left; UL, upper left; LR, lower right; UR, upper right.

that the activation of caspases precedes the beginning of sDF (46). The conclusion that apoptosis is the main mechanism responsible for sDF in the ejaculate was reinforced by the results obtained with cPARP, a different apoptotic marker (47,53), distributed among fragmented and nonfragmented sperm similarly to caspases.

The trigger of the apoptotic pathways can occur both in germ cells during spermatogenesis or after spermiation or both. Indeed, caspase activation and PARP cleavage have been observed both in the testis and in ejaculated sperm in response to apoptotic stimuli *in vitro* (12,50). The high percentage of sperm showing the simultaneous presence of sDF and both AB staining and active caspases or cPARP (present study), indicates that a large fraction of sperm concomitantly shows apoptotic traits and incomplete protamination, suggesting that apoptosis is triggered mostly in the testis. This conclusion is further supported by the presence of apoptotic bodies of testicular origin in semen of subfertile patients (20,31). However, the finding that the amount of sDF is greater in ejaculated sperm than in sperm extracted from the testis (14,15) indicates that apoptotic stimuli also can occur during transit in the male genital tracts. The fact that a fraction of live sperm also shows DNA fragmentation associated with active caspases is another indication that the onset of apoptosis may occur following release from the testis (see below for further discussion on this point).

In somatic cell apoptosis, the event responsible for the appearance of DNA nicks is the action of specific endonucleases (54). Studies on testis apoptosis demonstrate a similar action of endonucleases in germ cells (19,55), which are likely responsible for most apoptosis-associated DNA breaks found in ejaculated sperm (Figure 8). The action of endonucleases after spermiation (when chromatin is highly protamined), however, is less clear. The possible action of endonucleases in mature sperm has been questioned recently because of the architecture and strict compaction of the sperm nuclei (13,56). However, the presence of a nuclease able to cleave DNA has been clearly demonstrated in mature sperm (57,58) and the measurements by atomic force microscope reported that in mature compacted sperm nuclei there is sufficient space for potential protein functions (59). Moreover, chromatin compaction is still ongoing during epididymal transit, supporting the idea that apoptotic endonucleases can produce DNA breaks also after spermiation (Figure 8).

One of the hypothesized triggers of testis apoptosis is the impairment of sperm chromatin maturation (60). This idea is supported by the association between apoptotic markers and cell immaturity (24,46). A similar link also has been observed indirectly in our study, where more than 70% of the fragmented sperm show AB staining and about 80% and 50%, respectively, show active caspases and cPARP (Figures 4B,5B). Thus, a large amount of immature sperm with DNA fragmentation must also show apoptotic signs, further supporting the idea that an impairment of chromatin maturation, rather than representing a cause of sDF per se (because of lack of religation of DNA breaks) (9), can trigger apoptosis (60) (Figure 8). The large overlapping between sDF and sperm chromatin immaturity found in our study agrees with previous reports (24,28). Conversely, we did not find association between sDF and CK expression, considered another important sign of sperm immaturity (32,33). It should be mentioned, however, that a strict association between AB staining and CK was found by a previous study that also reported a larger percentage of CK-

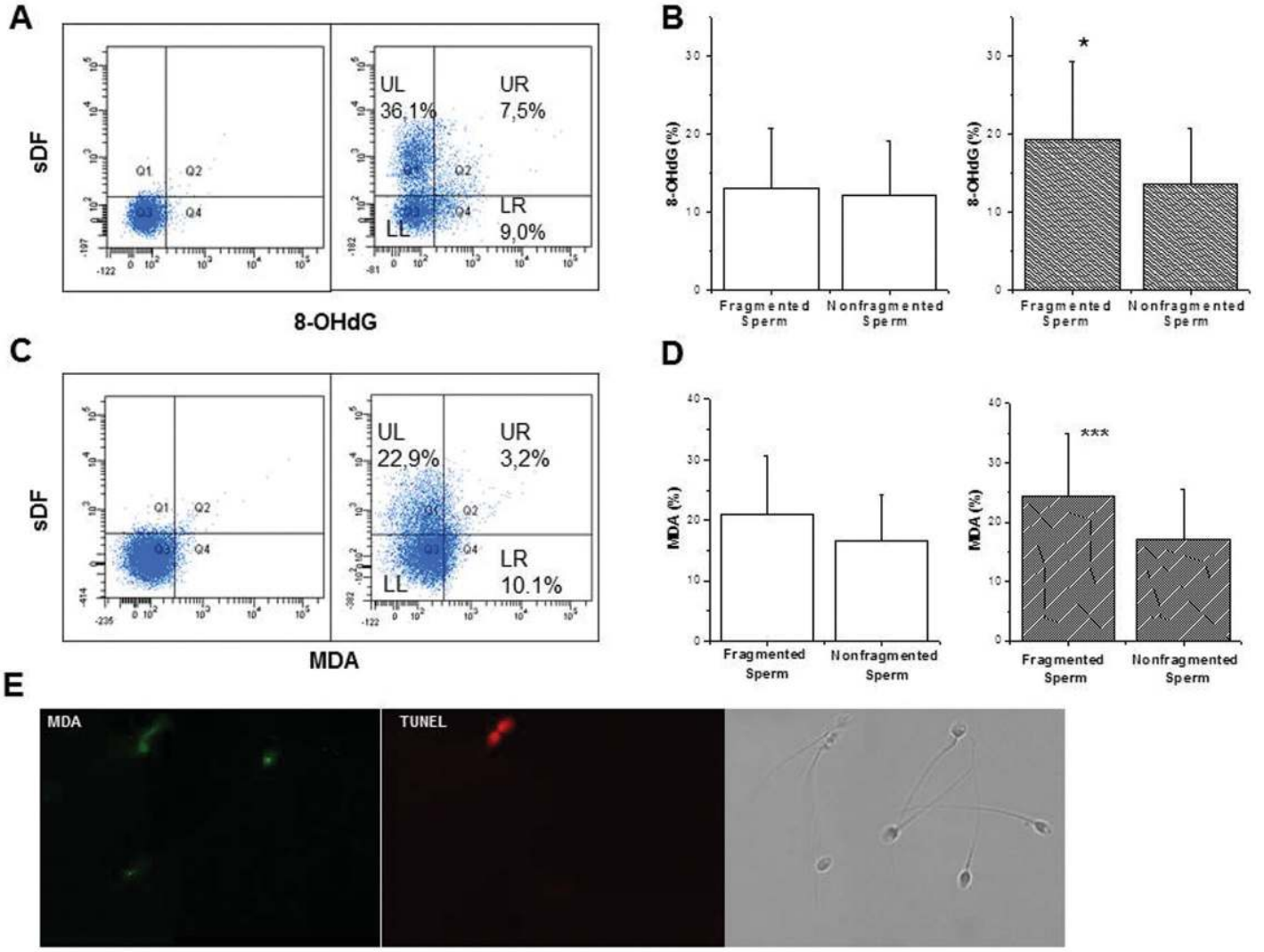

Figure 6. Concomitance of sDF and oxidative signs in human spermatozoa. 8-OHdG: (A) Dot plots of the negative control (left panel) and the corresponding test sample (right panel) showing the percentages of sperm without sDF and 8-OHdG (LL quadrant), sperm with sDF and without 8-OHdG (UL quadrant), sperm with sDF and 8-OHdG (UR quadrant) and sperm without sDF and with 8-OHdG (LR quadrant). Representative of 21 experiments. Percentages in the quadrants refer to the shown sample. (B) Percentage of sperm with 8-OHdG in fragmented (UR/(UR + UL)) and nonfragmented (LR/(LL + LR)) sperm, in total (left) and brighter (right) sperm population. MDA: (C) Dot plots of the negative control (left panel) and the corresponding test sample (right panel) showing the percentages of sperm without sDF and MDA (LL quadrant), sperm with sDF and without MDA (UL quadrant), sperm with sDF and MDA (UR quadrant) and sperm without sDF and with MDA (LR quadrant). Representative of 11 experiments. Percentages in the quadrants refer to the shown sample. (D) Percentage of sperm with MDA in fragmented sperm (UR/(UR + UL)) and nonfragmented (LR/(LL + LR)) sperm, in total (left) and brighter (right) sperm population. (E) Images from fluorescence microscopy showing the localization of MDA (left panel) in sperm with and without TUNEL labeling (middle panel). Right panel: bright field. Original magnification 1,000×. *$p <$ 0.05; ***$p < 0.001$. LL, lower left; UL, upper left; LR, lower right; UR, upper right.

expressing sperm (about 60%) (24) respective to our study (21.8%). Methodological aspects as well as patient selection (33) can explain the poor agreement about levels of expression of CK in human sperm present in the literature (24,33,61).

Oxidative attack is the third main mechanism hypothesized to induce sDF. We found that the occurrence of 8-OHdG and MDA, hallmarks of oxidative stress, scarcely mirrored the presence of sDF. A statistically significant association between oxidation and breakage in DNA was found only in brighter sperm, that is, excluding dead and DNA-fragmented dimmer sperm (44,45), suggesting that the role of oxidation in generating sDF might be masked by the high amounts of

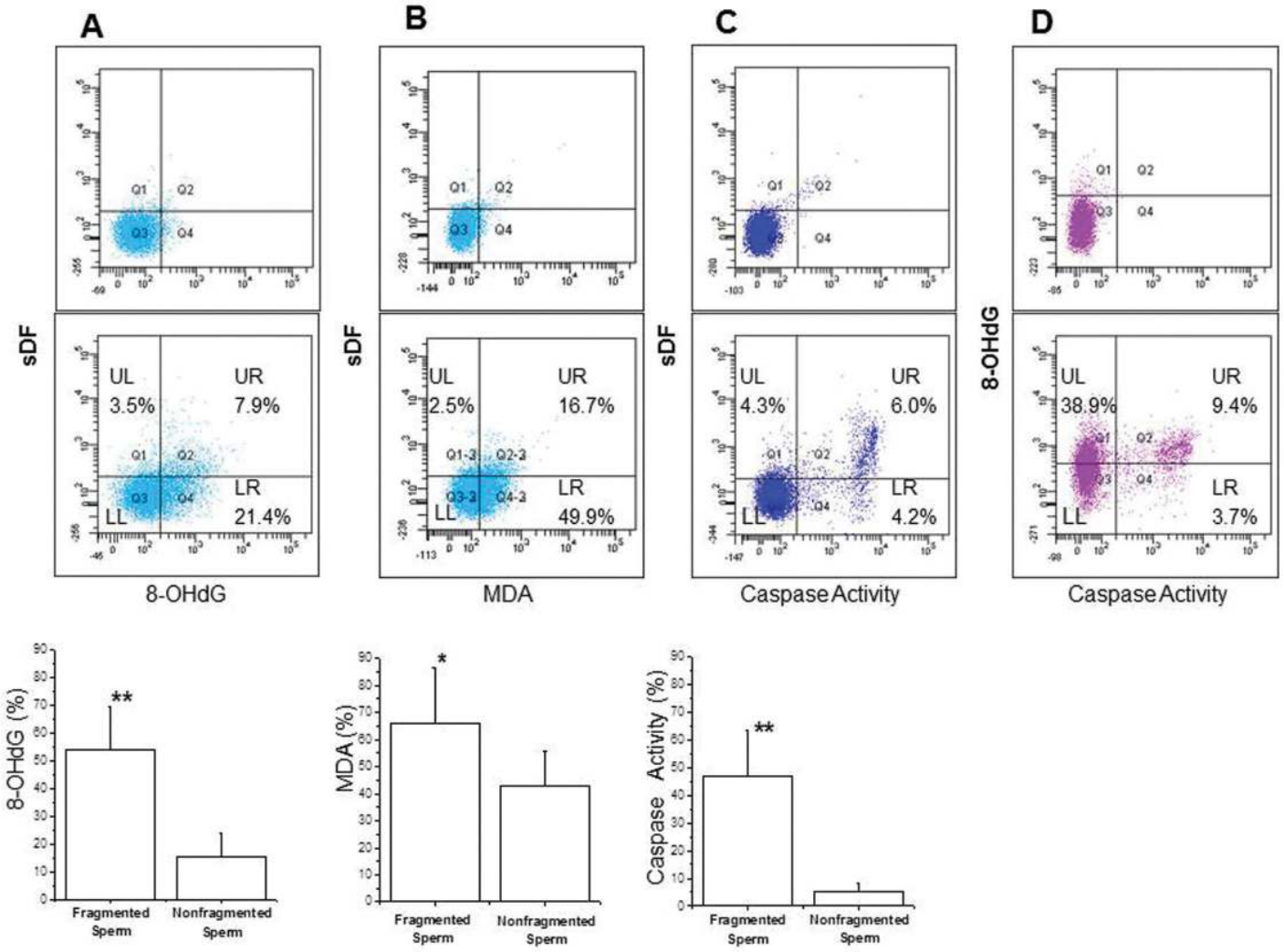

Figure 7. Experiments in live sperm. (A) Concomitance of sDF and 8-OHdG (n = 6). Dot plots of the negative control (upper panel) and the corresponding test sample (middle panel) showing percentage of: sperm without sDF and 8-OHdG (LL quadrant), sperm with sDF and without 8-OHdG (UL quadrant), sperm with sDF and 8-OHdG (UR quadrant), sperm without sDF and with 8-OHdG (LR quadrant). Representative of six experiments. Percentages in the quadrants refer to the shown sample. Lower panel, percentage of live sperm with 8-OHdG in fragmented (UR/(UR + UL)) and nonfragmented sperm (LR/(LL + LR)). (B) Concomitance of sDF and MDA (n = 6). Dot plots of the negative control (upper panel) and the corresponding test sample (middle panel) showing sperm without sDF and MDA (LL quadrant), sperm with sDF and without MDA (UL quadrant), sperm with sDF and MDA (UR quadrant) and sperm without sDF and with MDA (LR quadrant). Representative of six experiments. Percentages in the quadrants refer to the shown sample. Lower panel, percentage of live sperm with MDA in fragmented (UR/(UR + UL)) and nonfragmented sperm (LR/(LL + LR)). (C) Concomitance of sDF and active caspases (n = 7). Dot plots of the negative control (upper panel) and the corresponding test sample (middle panel) showing sperm without sDF and active caspases (LL quadrant), sperm with sDF and without active caspases (UL quadrant), sperm with sDF and active caspases (UR quadrant) and sperm without sDF and with active caspases (LR quadrant). Representative of six experiments. Percentages in the quadrants are referred to the shown sample. Lower panel, percentage of live sperm with active caspases in fragmented (UR/(UR + UL)) and nonfragmented sperm (LR/(LL + LR)). (D) Concomitance of 8-OHdG and active caspases (n = 3). Dot plots of the negative control (left panel) and the corresponding test sample (right panel) showing sperm without 8-OHdG and active caspases (LL quadrant), sperm with 8-OHdG and without active caspases (UL quadrant), sperm with 8-OHdG and active caspases (UR quadrant) and sperm without 8-OHdG and with active caspases (LR quadrant). Representative of three experiments. Percentages in the quadrants refer to the shown sample. *$p < 0.05$; **$p < 0.01$. LL, lower left; UL, upper left; LR, lower right; UR, upper right.

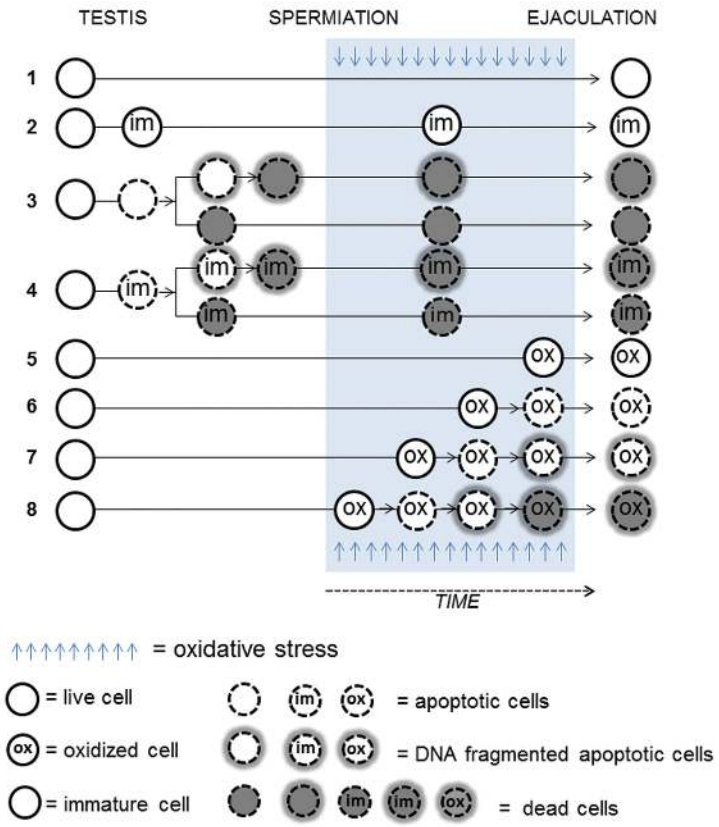

Figure 8. A scheme to summarize the results of the study. Lane 1: Live cells arriving in the ejaculate without DNA damage. Lane 2: Immature live cells arriving in the ejaculate without DNA damage. Lanes 3 and 4: Apoptotic cells evolving as DNA fragmented and dead (or directly dead). In Lane 4, apoptosis is induced by maturation impairment. These cells go through the genital tracts without being further DNA damaged by oxidative stress. Lane 5: Live cells undergoing oxidative damage just before ejaculation and thus not experiencing apoptosis. Lane 6: Live cells undergoing oxidative damage triggering apoptosis but not DNA fragmentation. Lane 7: Live cells undergoing oxidative damage triggering apoptosis and DNA fragmentation. Lane 8: Live cells undergoing oxidative damage triggering apoptosis, DNA fragmentation and death.

DNA-fragmented, dead sperm present in the ejaculates of subfertile men (35). This prompted us to investigate the mechanisms of sDF in only the viable sperm fraction of the ejaculate, where DNA damage is still ongoing. In live sperm, the frequency of the copresence of 8-OHdG and MDA with TUNEL positivity was much greater, highlighting a causative role of oxidation. The finding that caspase activation is present in fragmented live sperm with a similar frequency of 8-OHdG and MDA, and that most apoptotic sperm also show the oxidized base, supports the idea that ROS could produce DNA breaks through apoptotic routes (Figure 8) rather than by directly breaking the phosphodiester backbone. This is supported also by the large presence of cells with 8-OHdG but without DNA breaks and is consistent with studies reporting that ROS induce apoptotic pathways in mammalian spermatozoa during *in vitro* incubation (50,62–64).

Overall, our results depict a scenario (Figure 8) where apoptosis, either if primed in testis or after spermiation, is the main causative mechanism of sDF. In the testis, the impairment of chromatin maturation appears to be a relevant apoptotic stimulus, leading to sDF and/or cell death, consistent with the idea that apoptotic germ cells may escape phagocytosis by Sertoli cells, in postmeiotic phases (65). Oxidative stress does not seem to play a relevant role in producing sDF in testis, as also suggested by the scarce occurrence of 8-OHdG in testicular tissue (66), possibly due to the presence of efficient DNA repair systems (67). After spermiation, during the transit in the male genital tracts, oxygen species become relevant in triggering apoptosis in live cells (Figure 8), but seem ineffective toward dead/dying cells primed to apoptosis in testis (52) explaining why, in the bulk of ejaculated sperm where most DNA-fragmented cells are dead (35), the oxidative signs are scarcely associated to sDF.

Recently, it has been proposed that TUNEL is able to detect only sDF generated in peri/post mortem sperm, at the end of processes of destruction and after the induction of a self-perpetuating ROS production and activation of caspases by oxidative stress (7,13,36,68,69). According to this hypothesis, sperm DNA is damaged only by ROS which generate oxidized adducts to DNA, including 8-OHdG. However, if DNA-fragmented sperm were the final step of oxidative-injured cells, a large concomitance between 8-OHdG and MDA with DNA breaks should be observed, contrary to what this study found. In addition, we also found DNA breakage in a consistent percentage of live sperm, further questioning the interpretation of TUNEL positivity as a facet of moribund/dead sperm (13,36).

To the best of our knowledge, this is the first study investigating all the main mechanisms hypothesized for the origin of sDF by directly verifying the signs of such mechanisms in DNA-fragmented sperm. One limitation of the study is that the conclusions are mainly drawn on descriptive data, contrary to *in vitro* studies more suitable to trace cause–effect relationships between apoptotic/oxidative insults and sDF. However, it must be noted that *in vitro*-prepared sperm are scarcely representative of *in vivo* conditions and, as a result, are more vulnerable to oxidative as-

sault because they are deprived of the antioxidant defenses of seminal plasma (70). In addition, *in vitro* investigations cannot address the involvement of mechanisms thought to be triggered in the testis, such as apoptosis and sperm chromatin maturation defects, because these mechanisms are acting in cells maturing in the testis and during epididymal transit. Finally, it has to be considered that during *in vitro* incubation, sperm chromatin might undergo changes in accessibility of the tools to reveal sDF due to the removal of zinc from chromatin (71,72). Such events could affect chromatin stainability both in *ex vivo* study (like ours) and (with a greater extent) during *in vitro* incubations.

CONCLUSION

In conclusion, our results indicate that the main pathway leading to sperm DNA breaks is a process of apoptosis triggered by testicular conditions and by oxidative stress during the transit in the male genital tract. The clarification of the mechanisms leading to DNA breaks may help to better focus studies aimed at evaluating the effect of drugs for male infertility (for instance, the effect of antioxidants should be evaluated in live sperm) and open new therapeutic perspectives for the treatment of the infertile men.

ACKNOWLEDGMENTS

We are grateful to D Manganaro (Becton Dickinson, Milan, Italy) for precious technical assistance in the experiments of sorting spermatozoa. We also thank E Filimberti, S Degl'Innocenti and MG Fino (Azienda Ospedaliera-Universitaria Careggi), for evaluation of semen parameters. This study was supported by Regione Toscana (grant to G Forti), Ministry of Education and Scientific Research (PRIN 2009 project to E Baldi and FIRB project to S Marchiani).

DISCLOSURE

The authors declare they have no competing interests as defined by *Molecular Medicine*, or other interests that might be perceived to influence the results and discussion reported in this paper.

REFERENCES

1. Ahmadi A, Ng SC. (1999) Developmental capacity of damaged spermatozoa. *Hum. Reprod*. 14:2279–85.
2. Singh NP, *et al*. (1989) Abundant alkali-sensitive sites in DNA of human and mouse sperm. *Exp. Cell Res*. 184:461–70.
3. Gorczyca W, Traganos F, Jesionowska H, Darzynkiewicz Z. (1993) Presence of DNA strand breaks and increased sensitivity of DNA in situ to denaturation in abnormal human sperm cells: analogy to apoptosis of somatic cells. *Exp. Cell Res*. 207:202–5.
4. Tamburrino L, *et al*. (2012) Mechanisms and clinical correlates of sperm DNA damage. *Asian J. Androl*. 14:24–31.
5. Morris ID. (2002) Sperm DNA damage and cancer treatment. *Int. J. Androl*. 25:255–61.
6. Rubes J, *et al*. (2005) Episodic air pollution is associated with increased DNA fragmentation in human sperm without other changes in semen quality. *Hum. Reprod*. 20:2776–83.
7. Aitken RJ, Baker MA. (2013) Oxidative stress, spermatozoa and leukocytic infiltration: relationships forged by the opposing forces of microbial invasion and the search for perfection. *J. Reprod. Immunol*. 100:11–9.
8. Sakkas D, Manicardi G, Bianchi PG, Bizzaro D, Bianchi U. (1995) Relationship between the presence of endogenous nicks and sperm chromatin packaging in maturing and fertilizing mouse spermatozoa. *Biol. Reprod*. 52:1149–55.
9. Marcon L, Boissonneault G. (2004) Transient DNA strand breaks during mouse and human spermiogenesis new insights in stage specificity and link to chromatin remodeling. *Biol. Reprod*. 70:910–8.
10. Sakkas D, *et al*. (1999) Origin of DNA damage in ejaculated human spermatozoa. *Rev. Reprod*. 4:31–7.
11. Taylor SL, *et al*. (2004) Somatic cell apoptosis markers and pathways in human ejaculated sperm: potential utility as indicators of sperm quality. *Mol. Hum. Reprod*. 10:825–34.
12. Mahfouz RZ, *et al*. (2009) Evaluation of poly(ADP-ribose) polymerase cleavage (cPARP) in ejaculated human sperm fractions after induction of apoptosis. *Fertil. Steril*. 91:2210–20.
13. Aitken RJ, Bronson R, Smith TB, De Iuliis GN. (2013) The source and significance of DNA damage in human spermatozoa; a commentary on diagnostic strategies and straw man fallacies. *Mol. Hum. Reprod*. 19:475–85.
14. Greco E, *et al*. (2005) Efficient treatment of infertility due to sperm DNA damage by ICSI with testicular spermatozoa. *Hum. Reprod*. 20:226–30.
15. Moskovtsev SI, *et al*. (2010) Testicular spermatozoa have statistically significantly lower DNA damage compared with ejaculated spermatozoa in patients with unsuccessful oral antioxidant treatment. *Fertil. Steril*. 93:1142–6.
16. Sinha K, Das J, Pal PB, Sil PC. (2013) Oxidative stress: the mitochondria-dependent and mitochondria-independent pathways of apoptosis. *Arch. Toxicol*. 87:1157–80.
17. Oliva R. (2006) Protamines and male infertility. *Hum. Reprod. Update*. 12:417–35.
18. Almeida C, Sousa M, Barros A. (2009) Phosphatidylserine translocation in human spermatozoa from impaired spermatogenesis. *Reprod. Biomed. Online*. 19:770–7.
19. Shukla KK, Mahdi AA, Rajender S. (2012) Apoptosis, spermatogenesis and male infertility. *Front Biosci*. 4:746–54.
20. Lotti F, *et al*. (2012) Semen apoptotic M540 body levels correlate with testis abnormalities: a study in a cohort of infertile subjects. *Hum. Reprod*. 27:3393–402.
21. Wang X, *et al*. (2003) Oxidative stress is associated with increased apoptosis leading to spermatozoa DNA damage in patients with male factor infertility. *Fertil. Steril*. 80:531–5.
22. Guz J, *et al*. (2013) Comparison of oxidative stress/DNA damage in semen and blood of fertile and infertile men. *PLoS One*. 8:e68490.
23. Tarozzi N, *et al*. (2009) Anomalies in sperm chromatin packaging: implications for assisted reproduction techniques. *Reprod. Biomed. Online*. 18:486–95.
24. Sati L, *et al*. (2008) Double probing of human spermatozoa for persistent histones, surplus cytoplasm, apoptosis and DNA fragmentation. *Reprod. Biomed. Online*. 16:570–9.
25. Marchetti C, Gallego MA, Defossez A, Formstecher P, Marchetti P. (2004) Staining of human sperm with fluorochrome-labeled inhibitor of caspases to detect activated caspases: correlation with apoptosis and sperm parameters. *Hum. Reprod*. 19:1127–34.
26. Said T, *et al*. (2006) Selection of nonapoptotic spermatozoa as a new tool for enhancing assisted reproduction outcomes: an in vitro model. *Biol. Reprod*. 74:530–7.
27. Barroso G, Morshedi M, Oehninger S. (2000) Analysis of DNA fragmentation, plasma membrane translocation of phosphatidylserine and oxidative stress in human spermatozoa. *Hum. Reprod*. 15:1338–44.
28. De Iuliis GN, *et al*. (2009) DNA damage in human spermatozoa is highly correlated with the efficiency of chromatin remodeling and the formation of 8-hydroxy-2′-deoxyguanosine, a marker of oxidative stress. *Biol. Reprod*. 81:517–24.
29. Sakkas D, *et al*. (2002) Nature of DNA damage in ejaculated human spermatozoa and the possible involvement of apoptosis. *Biol. Reprod*. 66:1061–7.
30. Muratori M, Forti G, Baldi E. (2008) Comparing flow cytometry and fluorescence microscopy for analyzing human sperm DNA fragmentation by TUNEL labeling. *Cytometry A*. 73:785–7.
31. Marchiani S, *et al*. (2007) Characterization of M540 bodies in human semen: evidence that they are apoptotic bodies. *Mol. Hum. Reprod*. 13:621–31.
32. Huszar G, Vigue L. (1993) Incomplete development of human spermatozoa is associated with increased creatine phosphokinase concentration

and abnormal head morphology. *Mol. Reprod. Dev*. 34:292–8.
33. Cayli S, Sakkas D, Vigue L, Demir R, Huszar G. (2004) Cellular maturity and apoptosis in human sperm: creatine kinase, caspase-3 and Bcl-XL levels in mature and diminished maturity sperm. *Mol. Hum. Reprod*. 10:365–72.
34. World Health Organization. (2010) Laboratory Manual for the Examination and Processing of Human Semen. WHO Press, Geneva.
35. Mitchell LA, De Iuliis GN, Aitken RJ. (2010) The TUNEL assay consistently underestimates DNA damage in human spermatozoa and is influenced by DNA compaction and cell vitality: development of an improved methodology. *Int. J. Androl*. 34:2–13.
36. Smith TB, *et al*. (2013) The presence of a truncated base excision repair pathway in human spermatozoa that is mediated by OGG1. *J. Cell Sci*. 126:1488–97.
37. Aitken RJ, De Iuliis GN, Finnie JM, Hedges A, McLachlan RI. (2010) Analysis of the relationships between oxidative stress, DNA damage and sperm vitality in a patient population: development of diagnostic criteria. *Hum. Reprod*. 25:2415–26.
38. Marchiani S, *et al*. (2011) Sumo1-ylation of human spermatozoa and its relationship with semen quality. *Int. J. Androl*. 34:581–93.
39. Muratori M, *et al*. (2010) Small variations in crucial steps of TUNEL assay coupled to flow cytometry greatly affect measures of sperm DNA fragmentation. *J. Androl*. 31:336–45.
40. Cambi M, *et al*. (2013) Development of a specific method to evaluate 8-hydroxy, 2-deoxyguanosine in sperm nuclei: relationship with semen quality in a cohort of 94 subjects. *Reproduction*. 145:227–35.
41. Yang L, *et al*. (2009) Mice deficient in dihydrolipoyl succinyl transferase show increased vulnerability to mitochondrial toxins. *Neurobiol. Dis*. 36:320–30.
42. Marchiani S, *et al*. (2014) Characterization and sorting of flow cytometric populations in human semen. *Andrology*. 2:394–401.
43. Franken DR, Franken CJ, de la Guerre H, de Villiers A. (1999) Normal sperm morphology and chromatin packaging: comparison between aniline blue and chromomycin A3 staining. *Andrologia*. 31:361–6.
44. Muratori M, *et al*. (2008) Nuclear staining identifies two populations of human sperm with different DNA fragmentation extent and relationship with semen parameters. *Hum. Reprod*. 23:1035–43.
45. Marchiani S, *et al*. (2011) Sumo1-ylation of human spermatozoa and its relationship with semen quality. *Int. J. Androl*. 34:581–93.
46. Grunewald S, Sharma R, Paasch U, Glander HJ, Agarwal A. (2009) Impact of caspase activation in human spermatozoa. *Microsc. Res. Tech*. 72:878–88.
47. Agarwal A, *et al*. (2009) Potential biological role of poly (ADP-ribose) polymerase (PARP) in male gametes. *Reprod. Biol. Endocrinol*. 7:143.
48. Aziz N, Sharma RK, Mahfouz R, Jha R, Agarwal A. (2011) Association of sperm morphology and the sperm deformity index (SDI) with poly (ADP-ribose) polymerase (PARP) cleavage inhibition. *Fertil. Steril*. 95:2481–4.
49. Kemal Duru N, Morshedi M, Oehninger S. (2000) Effects of hydrogen peroxide on DNA and plasma membrane integrity of human spermatozoa. *Fertil. Steril*. 74:1200–7.
50. Lozano GM, *et al*. (2009) Relationship between caspase activity and apoptotic markers in human sperm in response to hydrogen peroxide and progesterone. *J. Reprod. Dev*. 55:615–21.
51. Rahman MB, *et al*. (2012) Oocyte quality determines bovine embryo development after fertilisation with hydrogen peroxide-stressed spermatozoa. *Reprod. Fertil. Dev*. 24:608–18.
52. Aitken RJ, *et al*. (2012) Electrophilic aldehydes generated by sperm metabolism activate mitochondrial reactive oxygen species generation and apoptosis by targeting succinate dehydrogenase. *J. Biol. Chem*. 287:33048–60.
53. Soldani C, Scovassi AI. (2002) Poly(ADP-ribose) polymerase-1 cleavage during apoptosis: an update. *Apoptosis*. 7:321–8.
54. Counis MF, Torriglia A. (2006) Acid DNases and their interest among apoptotic endonucleases. *Biochimie*. 88:1851–8.
55. Shaha C, Tripathi R, Mishra DP. (2010) Male germ cell apoptosis: regulation and biology. *Philos. Trans. R. Soc. Lond. B. Biol. Sci*. 365:1501–15.
56. Koppers AJ, De Iuliis GN, Finnie JM, McLaughlin EA, Aitken RJ. (2008) Significance of mitochondrial reactive oxygen species in the generation of oxidative stress in spermatozoa. *J. Clin. Endocrinol. Metab*. 93:3199–207.
57. Sotolongo B, Huang TT, Isenberger E, Ward WS. (2005) An endogenous nuclease in hamster, mouse, and human spermatozoa cleaves DNA into loop-sized fragments. *J. Androl*. 26:272–80.
58. Boaz SM, Dominguez K, Shaman JA, Ward WS. (2008) Mouse spermatozoa contain a nuclease that is activated by pretreatment with EGTA and subsequent calcium incubation. *J. Cell. Biochem*. 103:1636–45.
59. Oehninger S, *et al*. (2003) Presence and significance of somatic cell apoptosis markers in human ejaculated spermatozoa. *Reprod. Biomed. Online*. 7:469–76.
60. Sakkas D, *et al*. (2004) The presence of abnormal spermatozoa in the ejaculate: did apoptosis fail? *Hum. Fertil. (Camb)*. 7:99–103.
61. Jakab A, *et al*. (2003) Efficacy of the swim-up method in eliminating sperm with diminished maturity and aneuploidy. *Hum. Reprod*. 18:1481–8.
62. Grizard G, *et al*. (2007) In vitro alachlor effects on reactive oxygen species generation, motility patterns and apoptosis markers in human spermatozoa. *Reprod. Toxicol*. 23:55–62.
63. Martínez-Pastor F, *et al*. (2009) Reactive oxygen species generators affect quality parameters and apoptosis markers differently in red deer spermatozoa. *Reproduction*. 137:225–35.
64. Kang X, *et al*. (2012) Effects of hepatitis B virus S protein exposure on sperm membrane integrity and functions. *PLoS One*. 7:e33471.
65. Erenpreiss J, Spano M, Erenpreisa J, Bungum M, Giwercman A. (2006) Sperm chromatin structure and male fertility: biological and clinical aspects. *Asian J. Androl*. 8:11–29.
66. Ishikawa T, Fujioka H, Ishimura T, Takenaka A, Fujisawa M. (2007) Increased testicular 8-hydroxy-2′-deoxyguanosine in patients with varicocele. *BJU Int*. 100:863–6.
67. Morland I, *et al*. (2002) Human DNA glycosylases of the bacterial Fpg/MutM superfamily: an alternative pathway for the repair of 8-oxoguanine and other oxidation products in DNA. *Nucleic Acids Res*. 30:4926–36.
68. Aitken RJ, Baker MA. (2013) Causes and consequences of apoptosis in spermatozoa; contributions to infertility and impacts on development. *Int. J. Dev. Biol*. 57:265–72.
69. Aitken RJ, Smith TB, Jobling MS, Baker MA, De Iuliis GN. (2014) Oxidative stress and male reproductive health. *Asian J. Androl*. 16:31–8.
70. Smith R, Vantman D, Ponce J, Escobar J, Lissi E. (1996) Total antioxidant capacity of human seminal plasma. *Hum. Reprod*. 11:1655–60.
71. Björndahl L, Kvist U. (2010) Human sperm chromatin stabilization: a proposed model including zinc bridges. *Mol. Hum. Reprod*. 16:23–9.
72. Björndahl L, Kvist U. (2014) Structure of Chromatin in Spermatozoa. In: Baldi E and Muratori S, editors. *Genetic Damage in Human Spermatozoa*. Springer, New York. p 1–11.

Cite this article as: Muratori M, *et al*. (2015) Investigation on the origin of sperm DNA fragmentation: role of apoptosis, immaturity and oxidative stress. *Mol. Med*. 21:109–22.